Chapter 4 Methodology

4.1 408 MHz Allsky Survey

The observed data, which is optimum for this work, is obtained from the 408 MHz allsky survey of Haslam et al. after separation of its thermal component with the help of IRAS 60 micron emission (Broadbent et al.). At 408 MHz, there is very little absorption in the interstellar medium and the line of sight distribution of synchrotron emissivity was inferred mainly from its presumed relationship to the other tracers of spiral structure via these fitted free parameters. At lower frequencies, the absorption of synchrotron emission due to thermal electrons becomes significant and can give direct information of the non-thermal distribution along the line of sight. The allsky survey at 408 MHz was the result of four individual surveys. These surveys are summarized in Table 4.1.

All the surveys were made by using the nodding scan technique in which the telescope is fixed in azimuth along the meridian and nods up and down in elevation at a constant rate between the declination limits of the survey. The rotation of the earth provides the Right Ascension coverage. By applying an appropriate offset in the starting times of the scans from day to day, scan lines were made less than half a beam width

apart and each downward scan was crossed by regular upward scans allowing a consistent zero level to be set.

Table 4.1 The four surveys at 408 MHz (Haslam et al. 1982)

Telescope	Beam width (′)	Zone α	Zone δ
Jordrell 250 feet (Mark I)	48	0^h - 12^h Anticenter	-20°+ 60°
Effelsberg 100 meter	37	12^h - 04^h Northern Sky	-8°+ 48°
Parker 64 meter	51	0^h - 24^h Southern Sky	-90°+ 24°
Jordrell 250 feet (Mark IA)	48	0^h - 24^h North Polar Cap	+45°+ 90°

Each of the contributing surveys measured the left-hand circular polarized component. The synchrotron emission from a collection of cosmic ray electrons in a given magnetic field is about 70% linearly polarized perpendicular to the direction of the field. The observed radiation is generally less than 10% linearly polarized, however. This is partly due to the superposition of regions of emission in which the field runs in different directions but is mainly due to differential Faraday Rotation of the emission coming from various distances along the line of sight. Although the linearly polarized components of the radio continuum contain information about the magnetic field direction it is very difficult to interpret this from our position in the plane of the galaxy. Our present model deals only with the total intensity measurements.

The absolute zero levels and brightness temperature scales of the Northern Hemisphere surveys were calibrated using the 404 MHz survey of Pauliny-Toth & Shakeshaft (1962). This was an absolutely calibrated survey made of a grid of points with a 7.5m paraboloid. The grid point temperature had been measured relative to that of the North celestial pole and the pole temperature was found from a separate series of measurements. The 32° to 40° of declination overlap between the Parkes and Northern surveys allowed calibration of the former. The data of all the surveys were convolved to the same resolution of 51′. The error of the temperature scale of final allsky survey is believed to be less than 10% whilst the absolute zero level has an error of ±3 K. Positional pointing errors are ±1′ and are negligible compared with the beam width.

Before the galactic synchrotron emission can be modeled and fitted to the observations one has to remove extragalactic and thermal contributions. The cosmic background radiation has a temperature of 2.7 K. It is blackbody radiation and therefore contributes this amount to the Brightness Temperature at 408 MHz. Extragalactic radio sources, unresolved by the survey also provide an isotropic background. Lawson et al. (1987) estimates their contribution as 3.2 K. We have subtracted this total of 5.9 K from the survey values. In the galactic plane this is a rather insignificant contribution but near to the galactic poles where the observed temperature is ~20 K it is important.

4.2 Methodology

To demonstrate that the adapted model can describe the magnetic field of Milky Way Galaxy or not, we must compare the brightness temperatures from our model with the observational data. We have modified the model by as follow:

1. For the direction of any galactic longitude, ℓ in the galactic plane (b = 0°), the magnetic field component, which is perpendicular to the line of sight of the observers (on the Earth), $H_{\perp}$ is computed from the adapted model as equation (4.1). We choose the required parameters; the pitch angle, p = -8.2° and R_2 = 10.115 kpc from Han and Qiao' s work. Due to they concluded that the best fit parameter R_2 = 11.9 kpc for the position of the Sun is 10 kpc, certainly we rescale it by the factor 0.85

times. Also, we used the parameters R_0 = 11.0 kpc and R_1 = 1.91 kpc as in Sanguansak and used the offset constant C = 0.

Here,

$$H_{\perp} = H\cos(l + \theta + p) \tag{4.1}$$

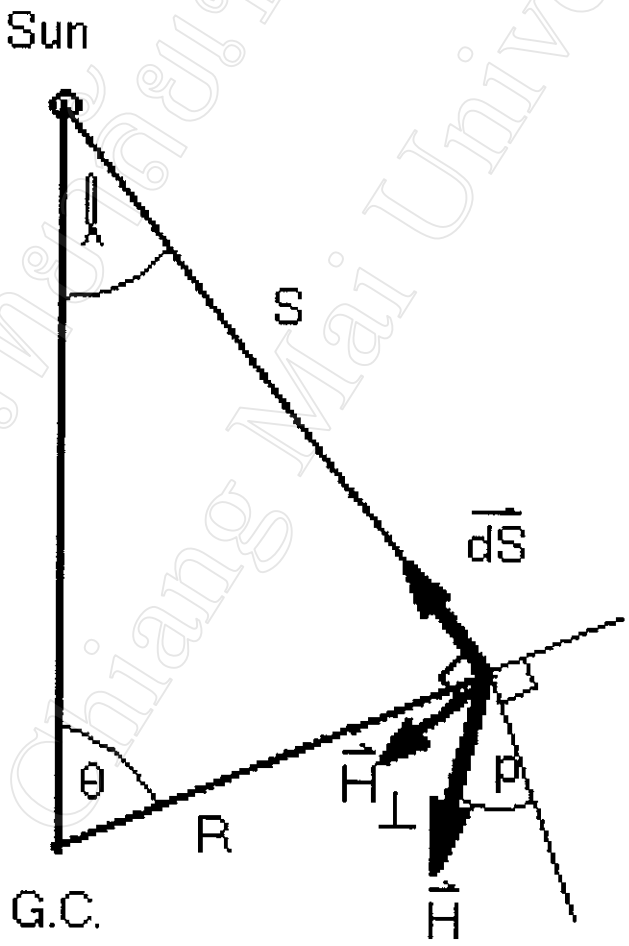

Figure 4.1 The coordinates of the galactic magnetic field show the component which perpendicular to the line of sight.

2. By equation (2.18), (2.24) and (2.25), we obtain the brightness temperatures, T_b in the ℓ direction.

3. In the same way, we get their values for every direction in the range of $-90° < \ell < 90°$. And then we carry them to plot graph of the brightness temperatures with the galactic longitude to compare with the observed brightness temperature at 408 MHz.

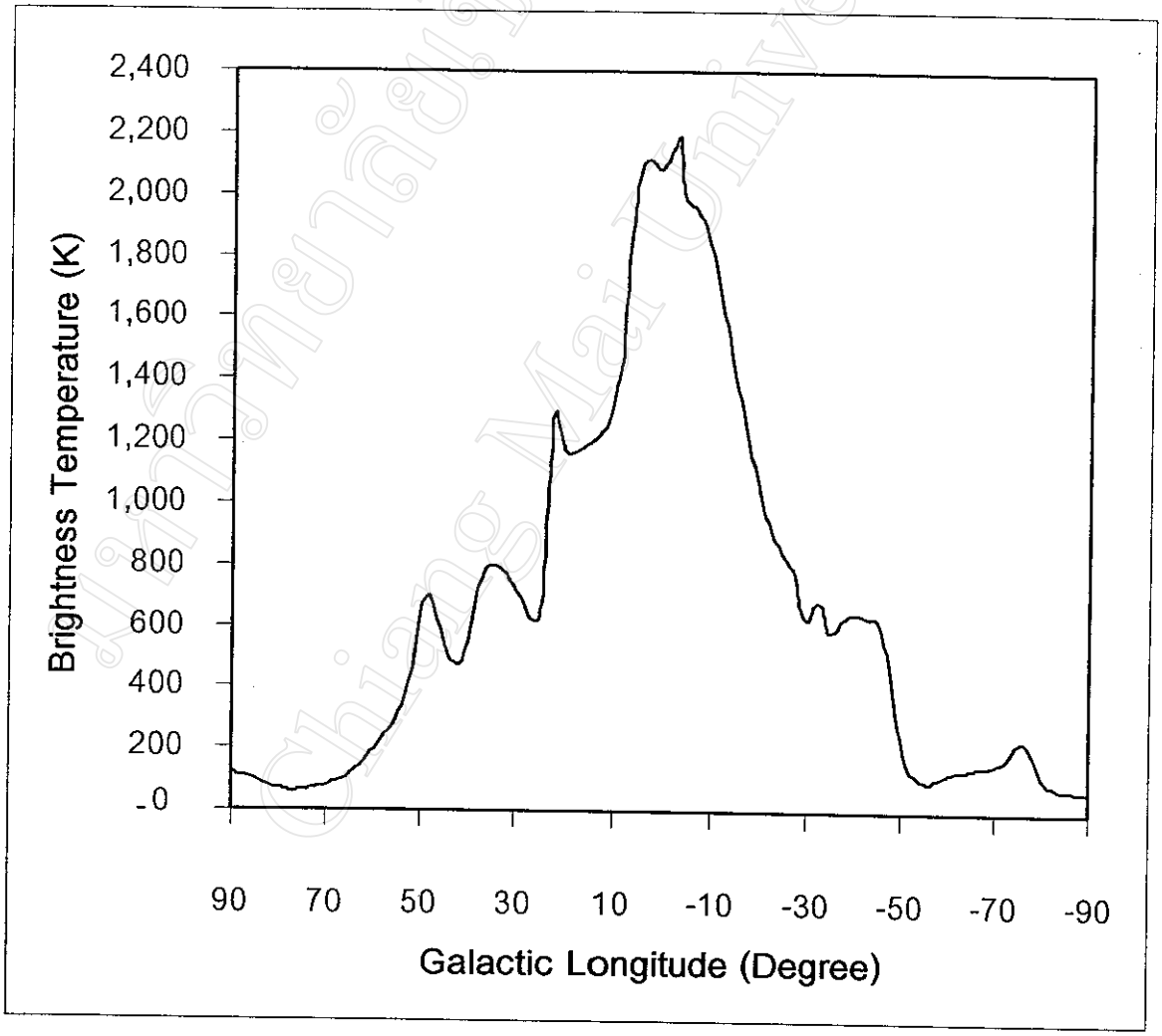

Figure 4.2 The calculated brightness temperature from the Adapted Model vary as the galactic longitudes in the range of -90° to 90° with the initial parameters.

4. From the result of comparison between the modeled and observed brightness temperatures at any galactic longitude, the profile was higher than the observational data. we analyzed and adjusted the parameters to find the optimized solution.

4.1 p and R_2 was adjusted to change the frequency of sinusoidal curve and the field strength in the galactic disk region as sinusoidal function effect to the brightness temperature all of ℓ direction for pushing down the profile to fit the observational data. We obtained the parameters p = -6.8° and R_2 = 9.35 kpc.

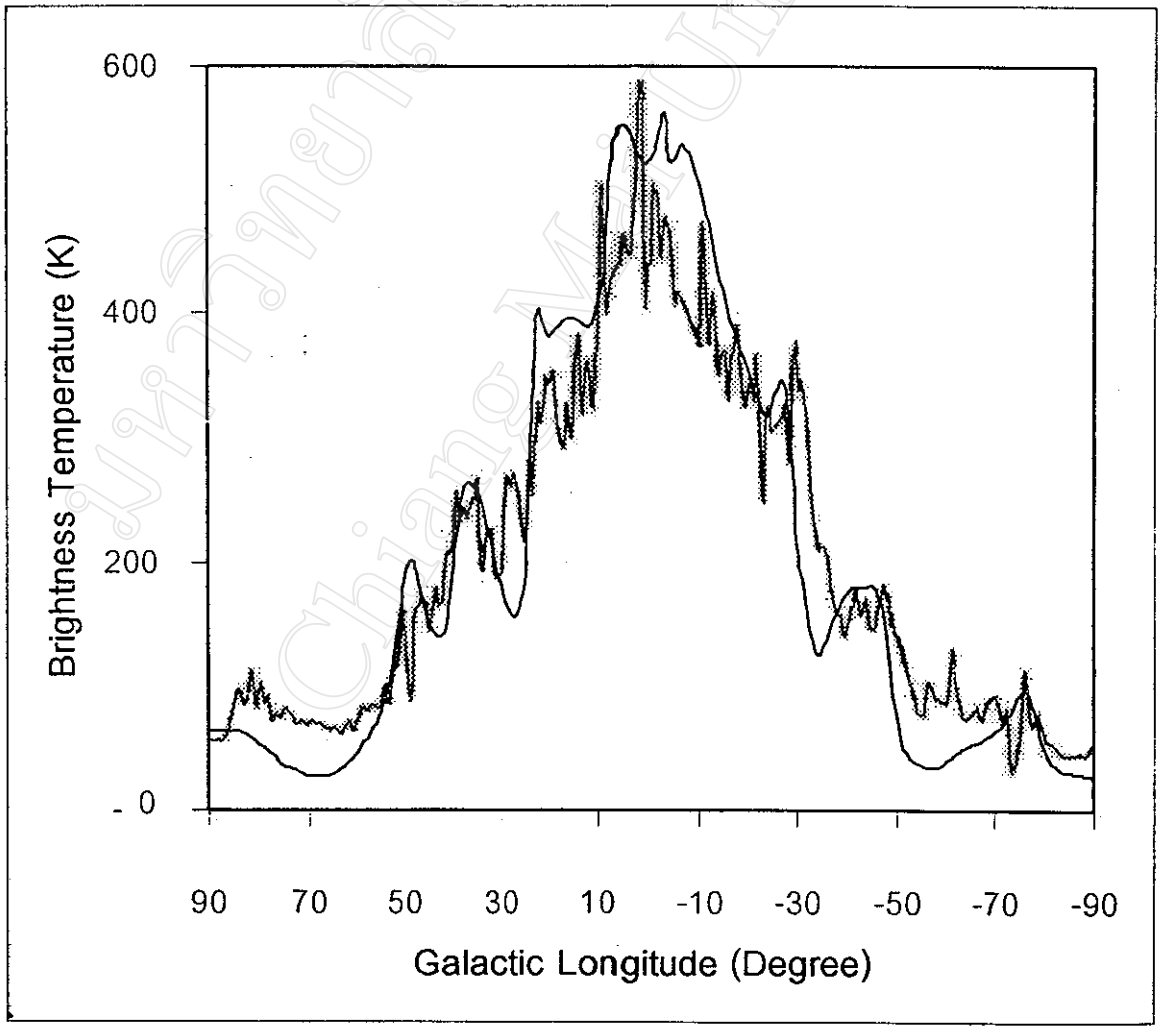

Figure 4.3 The profile with adjusted p = -6.8° and R_2 = 9.35 kpc.

4.2 While the profile was too high at some galactic longitude $|\ell| < \sim 25°$, but it is contrasted at the others. R_0 was adjusted to increase the field strength in the galactic disk region as exponential function, which effects to the profile all of ℓ direction. And R_1 was adjusted to decrease the field strength in the galactic center region effect to the profile at the small galactic longitude.

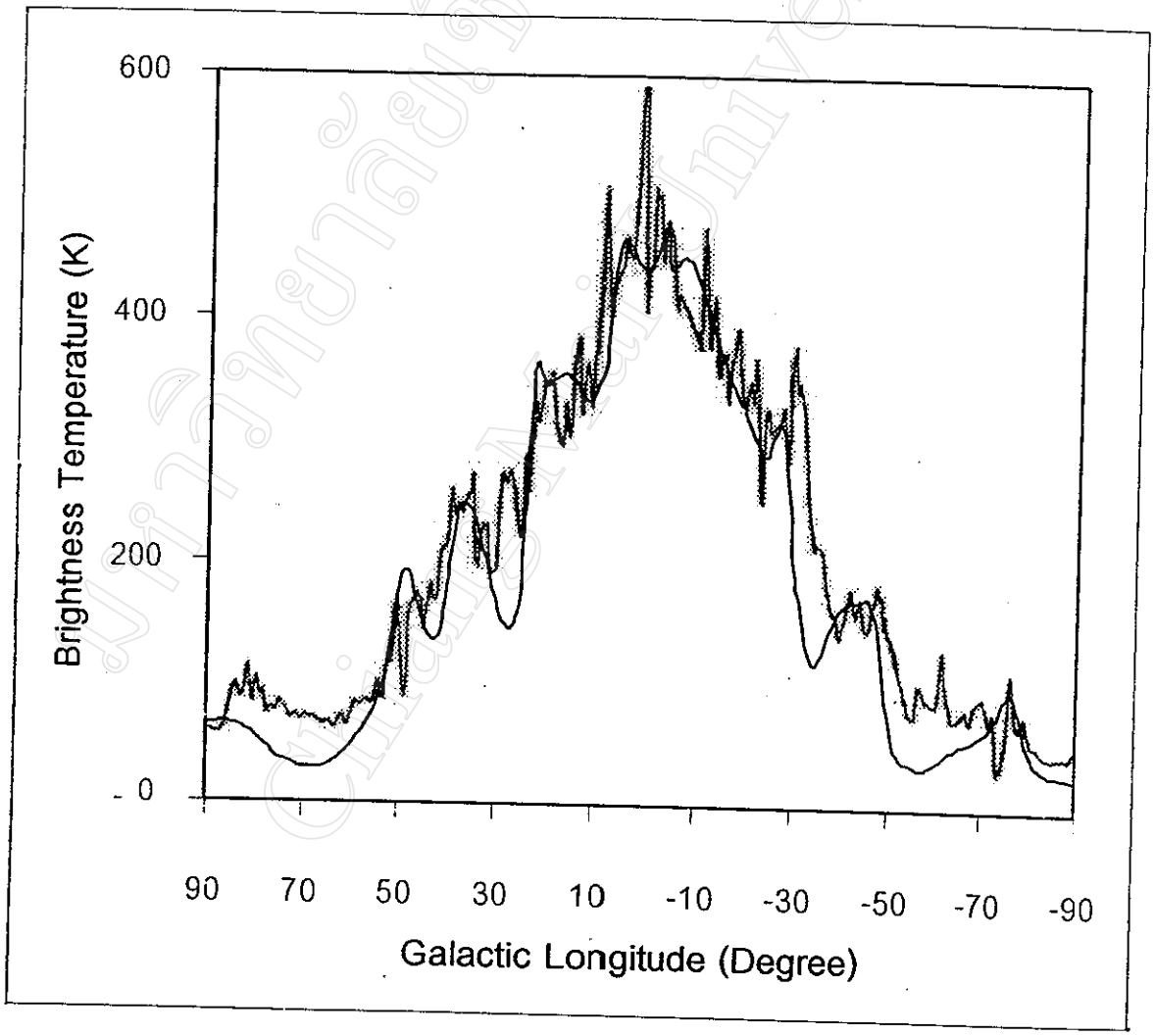

Figure 4.4 The profile with adjusted p = -6.8°, R_2 = 9.35 kpc, R_0 = 11.0 kpc and R_1 = 1.91 kpc .

4.3 At the galactic longitude that passes along the interarm region, for examples (-55°, -35°, 30° and 70°), the profile was lower than the observational data. Final adjusted parameter C, we believe that the field strength at the interarm region is not zero. We set the offset constant for the interarm region and we obtained C = 0.8 as shown in Figure 5.3.

5. The optimized solution can be analyzed and discussed to the adapted model has some significant for a description of the magnetic field of the Milky Way Galaxy in the next chapter.

Table 4.2 Summary of all the equations and their parameters for Synchrotron Model.

Quantity	Equation
Compression factor across an arm	$\rho_c = CR \cdot f(z) \cdot \exp\left(\frac{-0.5\alpha^2}{0.031}\right) + 1 \qquad CR = \begin{cases} 2.5 & ; \ 8.5\,kpc \le R \\ (12.75 - R)\cdot 0.5 & ; \ 8.5\,kpc \le R \le 12.75\,kpc \end{cases}$
Compression demodulation with z	$f(z) = \begin{cases} 1 + 0.908z - 23.529z^2 + 37.35z^3 & ; \ z \le 0.425\,kpc \\ 0 & ; \ z \ge 0.425\,kpc \end{cases}$
Electron flux density	$N_e\left(\frac{z}{z_0}\right) = 80x \begin{cases} 1.063 & \left(\frac{z}{z_0}\right) \le 0.2899 \\ 1.063 + 1.099\left(\frac{z}{z_0}\right) - 4.915\left(\frac{z}{z_0}\right)^2 + & \\ 4.307\left(\frac{z}{z_0}\right)^3 - 1.569\left(\frac{z}{z_0}\right)^4 + & \\ 0.256\left(\frac{z}{z_0}\right)^5 - 0.015\left(\frac{z}{z_0}\right)^6 & 0.2899 \le \left(\frac{z}{z_0}\right) \le 0.935 \\ 0.30788 - 0.0217\left(\frac{z}{z_0}\right) & 0.935 \le \left(\frac{z}{z_0}\right) \le 14.195 \\ 0 & \left(\frac{z}{z_0}\right) \ge 14.195 \end{cases}$ $z_0 = 0.591 - 0.0767R + 0.0147R^2$

Table 4.2 (Continued)

Quantity	Equation
Brightness Temperature	$T_b = 6.168 \times 10^4 \, \upsilon^{-2.8}$ $\times \int_0^S \left[N_e(s)\left(\rho_c(s) H_{reg}(s) \sin\theta\right)^{1.8} + 0.6861 N_e(s) \left(\frac{\rho_c(s) H_{reg}(s)}{F} \right)^{1.8} Y(s) \right] ds$
Irregular field realignment in arms	$Y(s) = 1 - 0.477 \left(\frac{\rho_c^2 - 1}{\rho_c^2} \right) \cdot \cos^2\theta$
Regular field	$H(R) = \left[1 - \exp\left(-2.768R^2\right)\right] \left[\exp\left(-\left(\frac{R}{R_0}\right)^2 \right) + \exp\left(-\left(\frac{R}{R_1}\right)^4 \right) \right]$ $R \le 3.4 \, kpc$ $H(R) = \left[1 - \exp\left(-2.768R^2\right)\right] \left[\exp\left(-\left(\frac{R}{R_0}\right)^2 \right) + \exp\left(-\left(\frac{R}{R_1}\right)^4 \right) \right] \cdot C$ $3.4 \, kpc \le R \le 12.75 \, kpc$ $and \quad \left| \cos\left(\theta + \beta \ln \frac{R}{R_2} \right) \right| \le C$ $H(R) = \left[1 - \exp\left(-2.768R^2\right)\right] \left[\exp\left(-\left(\frac{R}{R_0}\right)^2 \right) + \exp\left(-\left(\frac{R}{R_1}\right)^4 \right) \right] \cdot \cos\left(\theta + \beta \ln \frac{R}{R_2} \right)$ $3.4 \, kpc \le R \le 12.75 \, kpc$ $and \quad \left| \cos\left(\theta + \beta \ln \frac{R}{R_2} \right) \right| > C$ $\beta = \frac{1}{\tan p}$